[24]V. L. Ginzburg, Physica 24, S42 (1958).
[25]J. Bardeen, Phys. Rev. 94, 554 (1954).
[26]A. V. Bassewitz and G. V. Minnigerode, Z. Physik 181, 368 (1964).
[27]P. Cotti, E. M. Fryer, and J. L. Olsen, Helv. Phys. Acta 37, 585 (1964).
[28]I. Holwech and J. Jeppesen, Phil. Mag. 15, 217 (1967).
[29]R. Reich and F. Montariol, Compt. Rend. 254, 3357 (1962).
[30]A. Von Bassewitz and E. N. Mitchell, Phys. Rev. 182, 712 (1969).
[31]D. Markowtiz and L. P. Kadanoff, Phys. Rev. 131, 563 (1963).
[32]I. S. Khukhareva, Zh. Eksperim. i Teor. Fiz. 43, 1173 (1962) [Sov. Phys. JETP 16, 828 (1963)].
[33]M. Strongin, O. F. Kammerer, and A. Paskin, Phys. Rev. Letters 14, 949 (1965).
[34]E. P. Harris and D. E. Mapother, Phys. Rev. 165, 522 (1968).
[35]M. D. Maloney and F. de la Cruz, Solid State Commun. 9, 1647 (1971).
[36]L. P. Gorkov, Zh. Eksperim. i Teor. Fiz. 37, 883 (1959) [Sov. Phys. JETP 10, 593 (1960)].
[37]E. Helfand and N. R. Werthamer, Phys. Rev. 147, 288 (1966); Phys. Rev. Letters 13, 686 (1964).
[38]G. Eilenberger, Phys. Rev. 153, 584 (1967); Z. Physik 190, 142 (1966).
[39]G. W. Webb, Solid State Commun. 6, 33 (1968).
[40]P. C. Hohenberg and N. R. Werthamer, Phys. Rev. 153, 493 (1967).
[41]R. Koepke and G. Bergmann, Z. Physik 242, 31 (1971).
[42]W. D. Gregory, Phys. Rev. Letters 20, 53 (1968); W. D. Gregory, M. A. Superata, and P. J. Carroll, Phys. Rev. B 1, 85 (1971).
[43]To use the Ginzburg theory it is assumed that $\kappa(d_c) \simeq \kappa(\infty)$.
[44]R. T. Bate, B. Martin, and P. F. Mille, Phys. Rev. 131, 1482 (1963).
[45]The authors thank A. Baratoff for this suggestion.

PHYSICAL REVIEW B VOLUME 5, NUMBER 9 1 MAY 1972

Stability of Supercurrents in Cylindrical Films of Tin†*

H. Lawrence Phillips‡ and Hans Meissner
Department of Physics and Cryogenics Center, Stevens Institute of Technology, Hoboken, New Jersey 07030
(Received 7 September 1971)

Using current pulses with a rise time of less than 0.5 nsec and a pulse length of 240 nsec, the stability of supercurrents in cylindrical films of tin has been investigated. For current densities J in excess of the instability current density $J_I = J_I(0)\,[1-(T/T_c)^4]$, the sample voltage rises with time as $a(J,T)f(t/t')$, where $f(t/t')$ is a universal function of t/t'. The time constants t' cover a range of 0.5 nsec $< t' <$ 200 nsec. The amplitude coefficients a rise from zero as J exceeds J_I and then join onto the values $a = iR_n$, the voltage in the normal state. The time constants t' depend on current and temperature as $t' \approx t_0[J_I'/(J-J_I) - \epsilon J_I^2/(J-J_I)^2]$, where $J_I(0)$ has values of the order of 15×10^5 A/cm^2 and $t_0 \approx 14$ nsec, while $\epsilon \sim 3\times10^{-3}$.

I. INTRODUCTION

It has been found that for superconducting films there are three current densities of interest[1-4]: (i) a current density J_p at which flux tubes break free from their pinning sites with resulting flux flow and flux-flow resistivity; (ii) a current density J_I at which an instability occurs. The most prominent feature of this instability is the increase of the voltage along the film with time, even though the current is kept constant[1,3]; (iii) a current density J_c which is the theoretical critical current density as calculated from Ginzberg-Landau theory.[5] The present work deals with the instability current. Cylindrical samples were used since for flat samples there are two different types of instabilities, one which seems to be quite general and one arising from the edges of the film.[3] For cylindrical samples it is known[2] that there is only one instability down to 1.2 K. Also, with cylindrical samples it is possible to keep accidental perpendicular components of the magnetic field extremely low and therefore not to be disturbed by flux flow.

The first study of this instability[2] was restricted by the use of current pulses which had a ratio of pulse length to rise time of only 13. This prevented observation of the time constants over a sufficiently large range and had an uncontrolled influence on the early part of the voltage rise. In the present experiment the current pulse rises in less than 0.5 nsec and stays substantially constant for the rest of the pulse, 240 nsec. With this improvement it is now possible to show that all voltage V vs time t curves have the same shape: $V(t) = af(t/t')$, where the time constants t' cover a range of 0.5 nsec $< t' <$ 200 nsec, depending on current and temperature. The function $f(t/t')$ is similar to, but distinctly different from, the error

function expression used previously.[2] With this improved knowledge of the functional form of the voltage rise, it is now possible to study the dependence of the amplitude coefficient a on current and temperature. It is found that the amplitude coefficients a rise from zero at a finite current. The first onset of a provides a definition for the instability current J_I. For currents just slightly larger than J_I, the amplitude coefficients are small compared to the voltage for a normal conducting sample. Thus, there is a region where the instability does not rise to the normal state, but levels off at a smaller value. This is of great importance for future investigations because in this region it may be possible to study the structure of the sample at the instability. At the present there is no theoretical explanation for the instability. It has been made plausible that the instability is related to that found by Fink and Presson[6] for the superconducting surface sheath. These authors investigated theoretically the stability of the initially rather uniform current distribution with respect to a perturbation by which the current is sinusoidally deflected, being alternately closer to the outer or the inner surface. This type of instability is well known in plasma physics under the name "flute instability". Using only functions which are solutions to the Ginzberg-Landau equations, they find that the second variation $\delta^2\Omega$ of the free energy Ω has a minimum value if the modulation has a wavelength of $2\pi\xi$, where ξ is the coherence distance. If the resulting second variation $\delta^2\Omega$ is negative, the perturbations are growing. The growth rate can be found by entering these solutions into the time-dependent Ginzburg-Landau equations. The growth rate will be zero for $\delta^2\Omega$ zero and increase as $\delta^2\Omega$ becomes more and more negative. Unfortunately solutions for the growth rate remain one of the unsolved problems with this theory. It is beyond the purpose of this work to extend the theory to the present case and to evaluate the growth rates.

However, let us maintain the Fink-Presson theory as a working hypothesis. From their work we expect that for small currents $\delta^2\Omega$ is positive and the uniform supercurrent flow is stable. At a certain current J_I, $\delta^2\Omega$ becomes zero and, as the current is increased beyond this value, it becomes increasingly more negative, with increasingly faster growth rates and shorter and shorter time constants.

As the instability develops, the current density increases at those places where the current flow is pressed against the surface of the film. Either through phase slippage of the superconducting wave functions or because the current density reaches J_c at these places, a voltage appears. During this initial rise, entropy production is negligible. The word instability, as used here, refers to this initial process, which explains the nucleation of normal regions.

Subsequently, at later times, entropy production and energy storage become important. Offhand, one would expect that this would lead to extremely complicated processes, involving the time constants for the heat transfer from the film to the substrate, the heating of the substrate, etc. A simple estimate using one-dimensional temperature diffusion shows that in the longest time available—that of the current pulse—a temperature wave will travel into the substrate only over a distance of 10^{-4} cm, implying that the substrate is a rather poor heat sink. This may explain why a universal function $f(t/t')$ is found in the experiment. If t' is short compared to the other time constants considered above, then these time constants do not appear separately in the observed voltage rise.

A complete theory will not only have to explain the initial rise (which, we presume, follows from the ideas of Fink and Presson) but also the final shape of the $f(t/t')$ curve, which involves entropy production and energy storage.

The picture above is in accordance with the observation that flux flow is absent in the instability region. It is worth mentioning that a current J just slightly larger than J_I can be passed through the sample indefinitely without thermal runaway. Thus, while the flow through the whole sample is unstable, the presence of the normal regions stabilizes the flow, albeith with some energy dissipation.

Use of a large number of samples of various diameters has shown that the previous suggestion[2] that the time constants t' depend on total current rather than current density was spurious.

Use of a dual coaxial construction made it possible to have the magnetic field of the current either on the inside or on the outside of the sample film. This gave little change for the value of the observed time constants t', nor did it change the value of the amplitude coefficients a. This proves that the unevenness of the magnetic pressure occurring for a slightly eccentric internal current return is not responsible for the observed instability. (For a uniform, even though eccentric, external current return, the magnetic pressure on the sample film is uniform.)

II. EXPERIMENTAL ARRANGEMENT

The experimental arrangement is shown in Fig. 1. The current pulses are obtained by charging a coaxial rigid line ($Z = 50\ \Omega$, Phelps Dodge $\frac{1}{2}$-in. Spirafil) and discharging it through a coaxially mounted mercury relay. Two RC networks ahead of the relay sharpen and flatten the pulse and two capacitors on both sides of the relay compensate for its extra inductance. After a suitable delay,

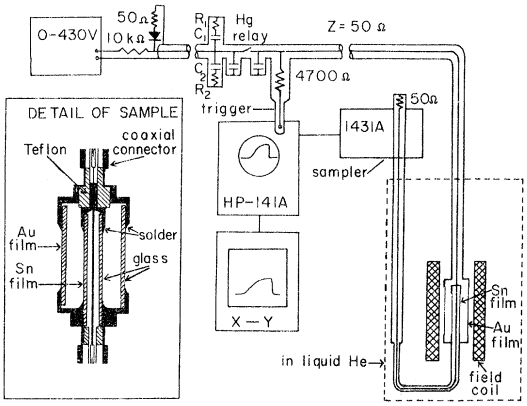

FIG. 1. Pulse circuitry. Insert: construction of sample mount.

the pulse is led to the cryostat and, using silver plated thin walled tubing, to the sample. It was found that the silver plating was the change which led to the most significant improvement of the rise time of the pulse.

The sample was made the common conductor of two coaxial systems, as shown on the insert of Fig. 1, which shows an outer and an inner coaxial system. One is used to lead the current pulse to the sample while the other is used to measure the voltage along the sample. A gold film is used for the outermost conductor, so that for all frequencies of interest the skin depth is larger than the thickness of the conductor and the current distribution is uniform, even for some eccentricity of the mount.

When the inner coaxial system is used for the current pulse, the magnetic field of the current is on the inside of the sample film. In this case eccentricity of the center conductor will lead to an uneven pressure of this magnetic field on the sample film, possibly giving cause to an instability.

When the outer coaxial system is used for the current pulse, the magnetic field is on the outside of the sample film and, since a gold film is used for the outermost conductor, it cannot exert an uneven pressure on the sample film. Most data were taken with this connection.

Since no difference was found in the response for "magnetic field inside" and "magnetic field outside," it was concluded that any residual unevenness of the pressure of the magnetic field arising from an eccentricity of the current is not important.

The coaxial system which is used for the pickup of the potential along the sample film is also connected to a $Z = 50$-Ω system which leads the voltage pulse through the Hewlett Packard Model 1431 A sampler to a 50-Ω termination.

By interchanging connections on top of the cryostat, it is possible to interchange the use of the inner and the outer coaxial system without interrupting the helium run.

With this construction, it is not possible to use a terminating resistor just ahead of the sample and the current pulse is reflected at the near short of the sample. Multiple reflections, however, were almost completely avoided through the use of a diode and a 50-Ω terminating resistor at the charging end of the delay line. The reflected pulse has negative polarity and is passed by the diode and dissipated in the 50-Ω resistor.

The voltage developed along the sample was displayed on the Hewlett Packard Model 141 A sampling oscilloscope and was recorded on a Hewlett Packard Model 135 A x-y recorder. Plots were restricted to records of the sample voltage as a function of the time. The same technique was used to record the voltage with the sample normal conducting at 4.2 K in order to obtain an indication of the current as a function of the time.

When the current pulse was brought directly through the sampler to a 50-Ω termination, the rise time was found to be approximately 0.1 nsec. With the sample in place, the rise time increased to approximately 0.5 nsec. For a normal sample film of length L, we expect a pulse, which originally had a rise time of $\Delta t_1 = b/c$ after being passed by the sample to the secondary system, to have a rise time of $\Delta t_2 = (2L + b)/c$ (c = phase velocity). With a sample length of $L = 3$ cm, we expect an increase of the rise time from 0.1 to 0.3 nsec. The remaining 0.2-nsec increase must then arise from absorption in the silver-plated thin-walled tubes leading the pulses in and out of the cryostat.

The cryostat was rather standard and was equipped with an electronic temperature control.[7] The temperature was evaluated from the vapor pressure using the 1958 ^{4}He scale.[8]

The earth's field was compensated for to less than 1%. A niobium-wound field coil in the liquid helium provided longitudinal magnetic fields for measuring the parallel critical fields of the sample film.

III. SAMPLES

The sample films of tin were vapor deposited onto the outside of cylindrical Pyrex substrates while liquid nitrogen was injected on the inside. A liquid-helium-filled trap ensured that even during vapor deposition the pressure did not rise above a few 10^{-7} Torr. The ends of the sample were reinforced with an extra layer of tin.

The gold films for the outermost conductors were also vapor deposited. In this case the substrates were fired with a thin coating of "Bright Platinum" (Englehard Industries No. 05) prior to deposition of the gold to reduce the danger of

damage during handling.

The details of the sample mount are shown on the insert of Fig. 1. The sample film was soldered into brass endpieces using Cerrolow No. 35 tin-indium alloy solder. This solder is superconducting up to 5.6 K. The gold films were soldered into place with pure indium solder. One of the ends is always free to slide through a Teflon spacer insuring freedom from axial stress. 50-Ω Microdot connectors were used for the electrical connections.

The dimensions of the samples and some of their relevant properties are given in Table I. Of the six samples used, four have approximately the same diameter of 1.68 mm. For three of these the film thickness was varied from 500 to 1700 Å. The fourth of these samples (No. 6) has the ratios of the diameters of the conductors chosen, so that the wave impedance is 100 Ω for the outer coaxial system, in effect introducing some extra inductance. All other ratios were chosen to give a wave impedance close to 50 Ω. The remaining two samples, Nos. 3 and 4, had sample diameters of 3.26 and 0.88 mm, respectively. Both had a film thickness of approximately 1000 Å. For details about sample 4 see below.

The critical temperature was defined by the extrapolation of the steep part of the transition curve to zero resistance, eliminating the lower transition temperature of the reenforced ends.

The critical field H_c was defined by the extrapolation of the transition curve in a parallel magnetic field to the normal resistance, eliminating the lower critical fields of the reenforced ends. $H_c(0)$ was obtained by extrapolation to zero temperature on an $H_c(T)$ vs T^2 plot. $H_c(0)$ depends strongly on film thickness and was used to find the film thickness, using data of Blumberg[9] and this laboratory.[10] In addition, the film thickness was obtained from the difference between the resistances $R_{300\ K}$ and $R_{4.2\ K}$, using a value of $\rho_{th}(300\ K) = 11.5\times10^{-6}\ \Omega$ cm.

The impurity mean free path was obtained using Dingle's[11] dependence of σ/σ_0 on d/l (σ_0 = bulk conductivity, σ = effective conductivity of a sample of thickness d, and impurity mean free path l) assuming diffuse boundary scattering. For the ratio σ_0/l, a value of $\sigma_0/l = 9.5\times10^{10}\ \Omega^{-1}\ \text{cm}^{-2}$ was used.[12]

Reasonable agreement was obtained for all samples except sample 4. This sample had an i.d. of the substrate of only 0.43 mm and, despite the use of a high-pressure liquid-nitrogen injection system, was apparently insufficiently cooled during vapor deposition of the tin. It was not quite as shiny as the other samples. The thickness calculated from the difference of $R_{300\ K} - R_{4\ K}$ was less than that obtained from $H_c(0)$ and less than that expected from the amount of tin evaporated. Also, the calculation

TABLE I. Dimensions and properties of samples.

Sample No.	Center conductor o.d. (mm)	Sample substrate i.d. (mm)	Sample film o.d. (mm)	Return substrate i.d. (mm)	Return film o.d. (mm)	Sample $R_{300\ K}$ (Ω)	Resistance $R_{4\ K}$[a] (Ω)	T_c (K)	Sample $H_c(0)$ (G)	Film thickness d Å[b]	Film thickness d Å[c]	Impurity mean free path l (Å)
1	0.508	1.40	1.68	3.76	5.72	8.4	0.74	3.882	1290	925	850	1700
2	0.508	1.40	1.66	3.76	5.72	4.0	0.325	3.824	610	1740	1800	1800
3	1.02	1.88	3.26	6.22	8.26	3.9	0.325	3.859	1240	955	950	1900
4	0.32	0.43	0.88	1.70	2.92	27.0	1.67	3.732	1080	1050	490	1000[d]
5	0.508	1.40	1.66	3.76	5.72	17.5	2.18	3.885	3500	545	430	2200
6	0.508	1.40	1.69	6.86	8.64	9.9	0.835	3.859	1590	800	720	2800

[a] $R_{4.2\ K}$ has been taken for the normal resistance R_n.

[b] From $H_c(0)$.

[c] From $R_{300\ K} - R_{4.2\ K}$.

[d] Using the thickness obtained from $H_c(0)$.

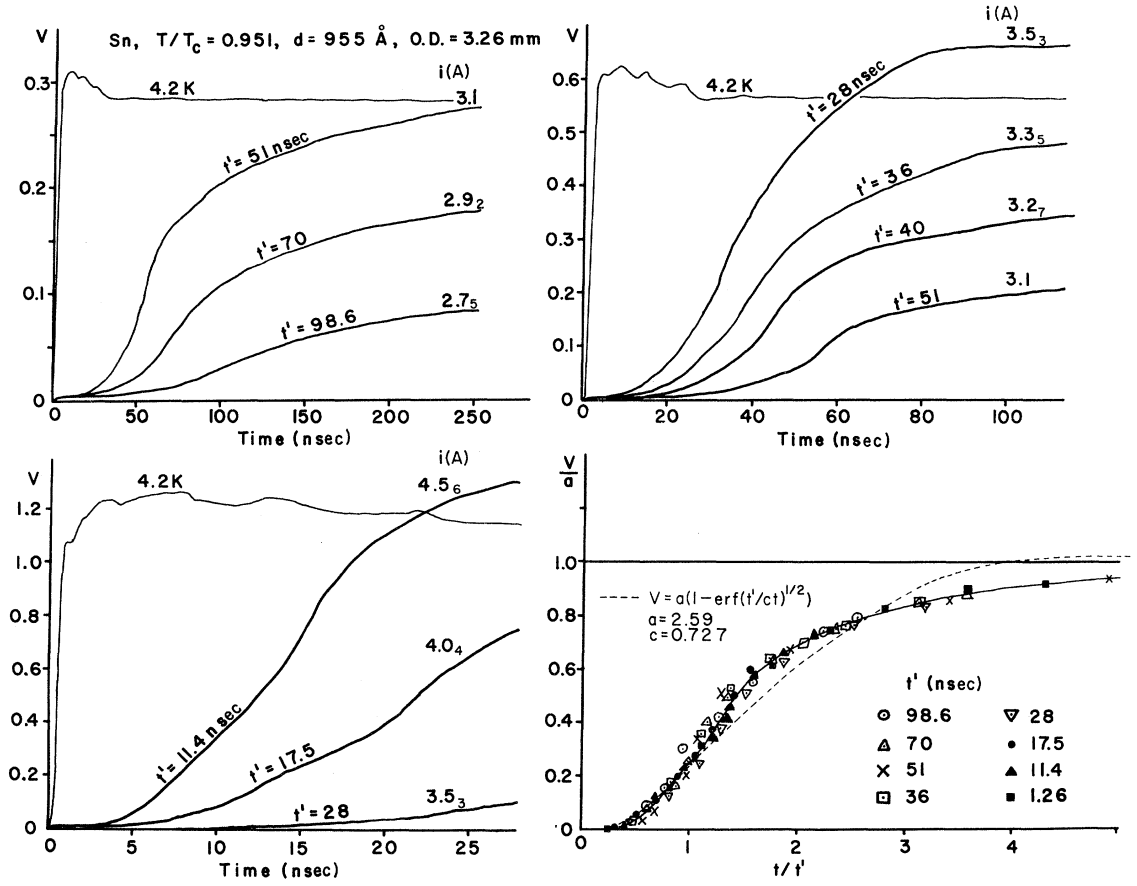

FIG. 2. Dependence of sample voltage on time and universal function $f(t/t')$. For details see text. (Connections for field outside.)

of the electronic mean free path gave reasonable values only if the thickness obtained from $H_c(0)$ was used. For this reason, we assume that sample 4 has a film thickness of approximately 1000 Å.

IV. EXPERIMENTAL RESULTS

A. Dependence of Sample Voltage on Time

Figure 2 shows plots of the sample voltage as a function of the time for sample three with $T/T_c = 0.951$. The time scale was changed from plot to plot, the amplitude of the current pulse was changed from trace to trace as indicated.

For comparison, the curves marked 4.2 K were taken with a normal conducting sample, using an arbitrary voltage scale, showing the approximate shape of the current pulse. In these latter plots, the finite pen speed produces an apparent increase of the rise time for the 0–100- and 0–250-nsec time scales. Only the plot with the 0–25-nsec time scale shows the front edge correctly. The increase of the rise time from 0.1 nsec (for the original current pulse) to 0.5 nsec (for the sample in place) can, for the most part, be explained by the finite length of the sample. The overshoot, however, cannot be explained in this way and is apparently caused by reflections at the connectors.

The curves shown on Fig. 2 were normalized by the choice of an amplitude coefficient a and a time constant t'. It was found that, by application of this normalization, all curves could be made to coincide rather closely, independent of current, temperature, film thickness, or sample diameter.

In the fourth field of Fig. 2, several points were taken from each of the curves shown and, after application of the normalization, plotted together to show the universal function $f(t/t')$. Table II gives a list of the values of the function $f(t/t')$ so defined. The time constants t' were chosen such that $f(1) = 0.25$.

For comparison, the error function expression used previously[2] is plotted in a way so as to coincide as much as possible with the present plot. It is to be noted that the error-function-type curve will keep rising until, eventually, it will reach a value of 2.59. This is the reason that in previous

TABLE II. Universal function $f(t/t')$.

t/t'	0.4	0.5	0.6	0.7	0.8	0.9	1.0
$f(t/t')$	0.037	0.05	0.075	0.105	0.14	0.187	0.250
t/t'	1.1	1.2	1.3	1.4	1.5	1.6	1.7
$f(t/t')$	0.33	0.397	0.46	0.51	0.56	0.60	0.63
t/t'	1.8	1.9	2.0	2.25	2.50	2.75	3.00
$f(t/t')$	0.655	0.695	0.705	0.757	0.795	0.82	0.845
t/t'	3.25	3.50	4.00	4.50	5.00	5.50	∞
$f(t/t')$	0.865	0.883	0.917	0.938	0.950	0.963	1.00

investigations the amplitude factors were too unreliable for use.

B. Amplitude Coefficient a and the Instability Current Density J_I

The curve with a pulse height of $i = 2.75$ A shown on Fig. 2. levels off at about 0.1 V, while, with $R_n = 0.325\ \Omega$ (see Table I, sample 3), one finds for the normal state $iR_n = 0.89$ V. This shows that the voltage rise does not always proceed to the value corresponding to the normal state resistance R_n.

This is studied in more detail in Figs. 3 and 4, which show plots of the reduced amplitude coefficient a/R_n as a function of the current density J for samples 5 and 3. For each temperature, there is a current density J_I below which no voltage will appear. As the current is increased above this "instability current density" J_I, the amplitude coefficient a approximately as $a_1(J-J_I)$ until the value $a = iR_n$ is reached. The line $a = iR_n$ is drawn in for comparison. Plots for some of the samples show a few data points above the line $a = iR_n$. In some cases these high-lying points can be corrected by a slightly different choice of t', although with some loss of match to the universal curve $f(t/t')$.

For samples 3 and 6, the current and voltage connections were interchanged and it was found that the value of the instability current density J_I was hardly affected (see Fig. 4), showing that the results are substantially the same for the magnetic field of the current on the inside or the outside of the film.

The values of J_I found from the a vs J plots are listed in Table III. They are found to be rather accurately proportional to $1-(T/T_c)^4$:

$$J_I = J_I(0)\,[1-(T/T_c)^4], \tag{1}$$

small existing differences being mostly due to the uncertainty in T_c. After weighing and averaging the individual values of $J_I(0)$ obtained from each temperature, it is found that $J_I(0)$ still varies from sample to sample, covering a range of 8.75×10^5 A/cm^2 $< J_I(0) < 20\times10^5$ A/cm^2.

The $1-(T/T_c)^4$ temperature dependence is the same as that λ^{-2} where λ is the superconducting penetration depth. According to Miller and Cody,[13] λ^2 depends on film thickness d as

$$\lambda^2 = \lambda_0^2(1+420/d), \tag{2}$$

where d is measured in Å. This suggests correcting the values of $J_I(0)$ by including a factor $1+420/d$. This does not reduce the over-all spread of the data significantly, showing that other effects, for instance the state of the surface, have more influence on $J_I(0)$ than this factor. (See Table III.) We have checked for other dependences of $J_I(0)$ on sample diameter, film thickness, and resistivity and we could not find any systematic dependence which was discernible above the general scatter of the data.

C. Time Constants t'

Values of t' vary from 0.5 to 200 nsec, with the shortest time constants occurring at the highest current densities. The time constants become very large as J is lowered to J_I and it seems reasonable to assume that the time constants go to infinity as

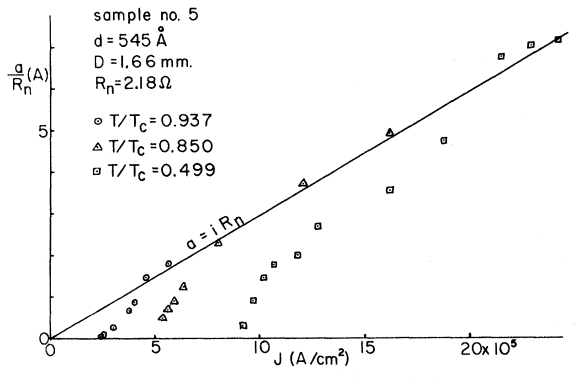

FIG. 3. Dependence of the reduced amplitude coefficient a/R_n on current density J, sample 5. Along the line $a = iR_n$ the sample voltage attains the value expected for a normal conducting sample. (Connections for field outside.)

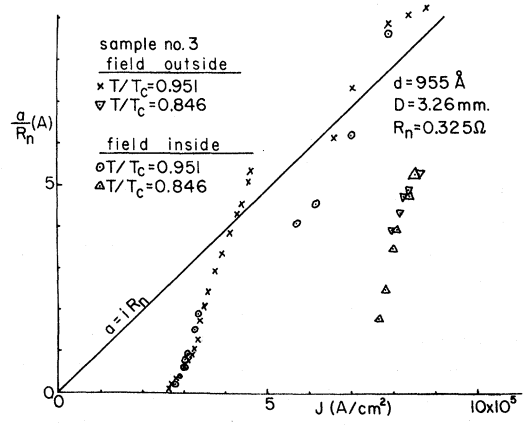

FIG. 4. Dependence of the reduced amplitude coefficient a/R_n on current density J, sample 3. Note the second set of data points for connections with field inside.

J approaches J_I from above. This suggests that t' is a function of $J-J_I$ rather than of J.

In the absence of a theory, it is difficult to decide in which fashion to plot the data. Previous plots[2] have shown $\ln t'$ plotted as a function of $J/[1-(T/T_c)^4]$.

Here, we found that a plot of t' as a function of $J_I/(J-J_I)$ brought most of the data quite close together. It appears that plots of this type are extremely sensitive to the choice of J_I. Since the error limits of the values of J_I obtained from the onset of $a(J, T)$ are rather wide, J_I was adjusted slightly, mostly to somewhat lower values for the t' vs $J_I/(J-J_I)$ plot. It is felt that the values of J_I so determined are more accurate than those obtained from the $a(J, T)$ plot. With this adjustment, most of the data points could be made to fall on a line

$$t' = t_0 J_I/(J-J_I), \tag{3}$$

with $t_0 \approx 14$ nsec. However, there were always a few points, very close to J_I, which could not be made to fit this linear relation. This suggests the existence of a small second term:

$$t' = t_0 [J_I/J - J_I) - \epsilon J_I^2/(J-J_I)^2], \tag{4}$$

with $\epsilon \approx 3\times 10^{-3}$. The choices of t_0 and J_I for best fit are not quite independent of each other. However, a detailed analysis did not seem to be warranted at this time and a constant value of $t_0 = 13.9$ nsec was used, although the true value of t_0 may vary somewhat from sample to sample.

Figure 5 shows plots of t' as a function of $J_I(J-J_I)$ for all the six samples used here. In order to omit confusion, the plots have been shifted by a constant amount of $J_I/(J-J_I) = 0.4$ against each other. It is apparent that the resulting plots are quite similar and that the choice of t_0 is rather accurate for most samples. Samples 5 and 6 would have given a somewhat better fit to Eq. (4) if t_0 had been chosen smaller and J_I had been slightly larger.

The resulting values of J_I are entered in Table III for comparison with those obtained from the onset of the amplitude coefficients a.

It should be pointed out that the data in Fig. 5 do not point toward $J_I/(J-J_I) = 0$ but rather to a finite value. It is surmised that this finite value is $J_I/(J_c-J_I)$, where J_c is the critical current density.[5] If the critical current density is exceeded, one would expect that the samples switch in about 10^{-12} sec (somewhat dependent on temperature), which is still much shorter than the time constants observed here. In any case, one would not expect the data to follow Eq. (4) in a region where J approaches J_c. Deviations of this type are more apparent on a plot of $\ln t'/t_0$ as a function of $\ln(J_I/(J-J_I)$ (see Fig. 6), which shows that deviations on account of the term $\epsilon J_I^2/(J-J_I)^2$ are hardly notice-

TABLE III. Instability current density.

		Instability current density J_I				$J_I(0) = J_I/(1-(T/T_c)^4)$			
		field outside		field inside		field outside		field inside	
Sample No.	T/T_c	from t' (10^5 A/cm^2)	from a (10^5 A/cm^2)	from t' (10^5 A/cm^2)	from a (10^5 A/cm^2)	from t' (10^5 A/cm^2)	from a (10^5 A/cm^2)	from t' (10^5 A/cm^2)	from a (10^5 A/cm^2)
1	0.950	2.52	2.70	...	...	13.6	14.6	...	...
	0.845	9.48	10.2	...	...	19.3	20.8	...	...
	0.772	11.79	13.5	...	...	18.3	20.9	...	...
				$\langle J_I(0)\rangle$[a]		17.7	19.6	...	...
2	0.948	3.17	3.4	...	...	16.5	17.7	...	...
	0.852	7.11	7.7	...	...	15.0	16.3	...	...
				$\langle J_I(0)\rangle$		15.6	16.8	...	...
3	0.951	2.48	2.55	2.80	2.65	13.6	14.0	15.4	14.6
	0.846	6.96	6.5	7.57	7.5	14.3	13.3	15.5	15.4
				$\langle J_I(0)\rangle$		14.0	13.6	15.5	15.1
4	0.943	1.52	2.2	...	...	7.3	10.5	...	...
	0.838	5.09	5.2	...	...	10.0	10.3	...	...
	0.527	8.0	8.8	...	...	8.7	9.5	...	...
				$\langle J_I(0)\rangle$		8.76	9.68		
5	0.937	1.88	2.1	...	...	8.2	9.2	...	...
	0.850	4.97	4.8	...	...	10.4	10.0	...	...
	0.499	8.49	8.8	...	...	9.1	9.4	...	...
				$\langle J_I(0)\rangle$		9.2	9.46	...	...
6	0.923	4.44	4.9	4.33	4.8	16.2	17.9	15.8	17.5
	0.832	8.92	10	7.65	9	17.1	19.2	14.7	17.3
				$\langle J_I(0)\rangle$		16.8	18.7	15.1	17.4

[a]Weighted average, assuming that T_c is uncertain by 0.015 K.

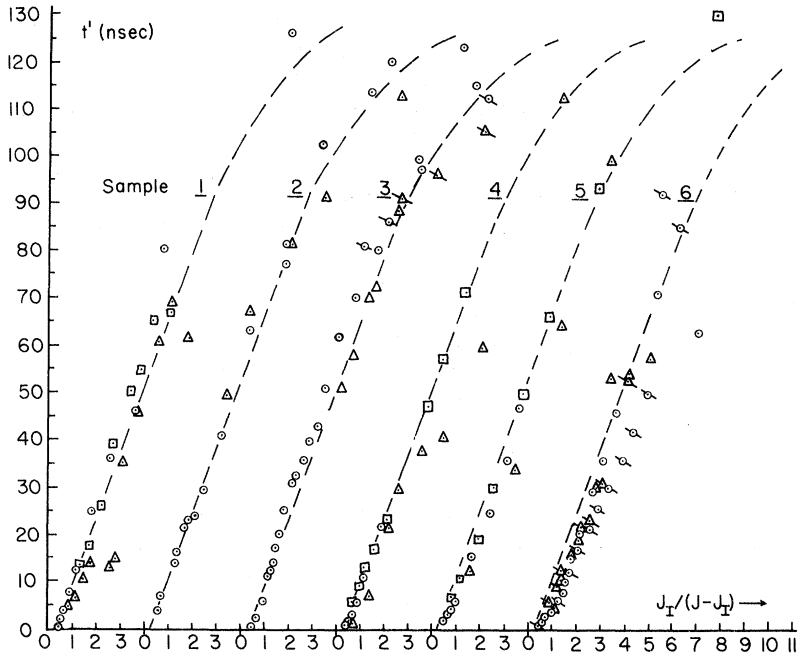

FIG. 5. Dependence of the time constants t' on $J_I/(J-J_I)$. The curves have been shifted by constant amounts of $J_I/(J-J_I)=0.4$ against each other. ⊙ ≈ $0.95T/T_c$; △ ≈ $0.85T/T_c$; ⊡ ~lowest temperature, all with the field outside connection. ⊙, △, and ⊡ with field inside connection. The exact temperatures are given in Table III.

able on this plot, but deviations for large J, where effects of J_c may come into play, are quite noticeable.

Figure 5 also shows that the data points for the field inside can be made to coincide with those for the field outside with only a slightly different choice of J_I. For sample 3 this required a slight lowering of J_I (as one might expect from an additional source for the instability) but for sample 6 it required a slight increase of J_I. We conclude that this small change in J_I is due to slightly different surface conditions and that the unevenness of the pressure of the magnetic field from the current return is not important.

V. COMPARISON WITH OTHER EXPERIMENTS

Quite similar experiments have been performed either from the point of view of critical currents[14] or of switching times.[15] As far as we know, there is only one determination of the true critical current, by Hunt,[16] who used samples less than 2 μm wide, which apparently are stable up to the true critical current. Most other investigations of "critical currents in thin films" determined either the instability currents investigated here or the depinning current J_P. The latter is determined if there are residual perpendicular components of the magnetic field; J_P has the same temperature dependence as J_c but is much smaller. By omitting edges and careful choice of the current return as well as compensation of the earth's magnetic field, it was possible to minimize flux-flow resistance effects so that they are vanishingly small and are not visible. The combined effects of flux flow and instability have been studied in Ref. 3.

VI. CONCLUSIONS

Cylindrical film samples with concentric current

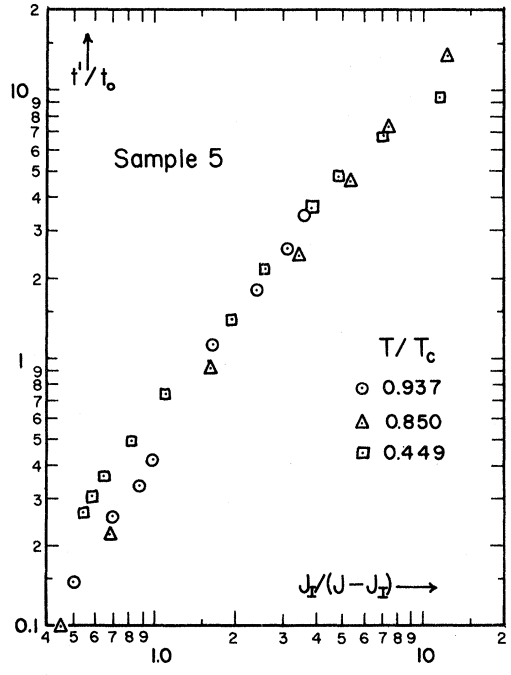

FIG. 6. Logarithmic plot of the dependence of t'/t_0 on $J_I/(J-J_I)$ with $t_0 \approx 13.9$ nsec.

return were subjected to roughly square current pulses. In the temperature range $0.5 < T/T_c < 0.95$, it was found that, as the current density exceeds the instability current density $J_I = J_I(0)\,[1-(T/T_c)^4]$, an instability develops. This instability manifests itself as a voltage rise which is given by $V(t) = a(J, T) f(t/t')$, where $f(t/t')$ is a universal function.

The amplitude coefficients a rise from zero as J exceeds the instability current density J_I. For somewhat larger currents the amplitude coefficients join onto the value expected for a normal sample: $a = iR_n$.

The time constants t' cover a range 0.5 nsec $< t' <$ 200 nsec. They depend on current and temperature, on the latter only through the temperature dependence of J_I, as

$$t' = t_0\,[J_I/(J - J_I) - \epsilon J_I^2/(J - J_I)^2].$$

It appears remarkable that neither $V(t)$ nor $t'(J, J_I)$ show any irregularities in their functional behavior as the amplitude coefficient a changes from values smaller than that corresponding to the normal-state resistance to $a = iR_n$, i. e., whether the final state of the sample is the intermediate state or the fully normal state.

As a working hypothesis, it is assumed that the instabilities observed here are similar to the flute-type instability (well known in plasma physics) as described by Fink and Presson for the superconducting surface sheath.

ACKNOWLEDGMENTS

This work was supported in part by the National Science Foundation and in part by the Stevens Cryogenics Center through a Grant from the DOD Themis program. The authors are grateful to Dr. George Schmidt and to Dr. Harold Salwen for their help with the evaluation of the system response. The authors are grateful to the Office of Naval Research for the supply of helium gas and to Gunther Wirth for the operation of the helium liquefier and for technical assistance.

---

†Supported in part by the National Science Foundation, in part by the Cryogenics Center through a grant from the DOD Themis Program.

‡Now at the University of Karlsruhe, Germany.

*Based in part on a thesis submitted by H. L. P. to Stevens Institute of Technology in partial fulfillment of the requirements for the Ph. D. degree.

[1]P. Tholfsen and H. Meissner, Phys. Rev. 185, 653 (1969).

[2]H. Meissner, J. Low Temp. Phys. 3, 563 (1970).

[3]H. Meissner and P. Tholfsen, J. Low Temp. Phys. 4, 141 (1971).

[4]H. Meissner, in *Proceedings of the Twelfth International Conference on Low Temperature Physics*, edited by Eizo Kanda (Academic Press of Japan, Keigaku Publishing Co. Ltd., Tokyo, Japan, 1971), p. 493.

[5]V. L. Ginzburg, Dokl. Akad. Nauk SSSR 118, 464 (1958) [Sov. Phys. Doklady 3, 102 (1958)].

[6]H. J. Fink and A. G. Presson, Phys. Rev. B 1, 1091 (1970).

[7]H. Meissner, Phys. Rev. 109, 668 (1958).

[8]H. Van Dijk, M. Durieux, J. R. Clement, and J. K. Logan, Natl. Bur. Std. (U.S.) Monograph No. 10 (U. S. GPO, Washington, D. C., 1960).

[9]R. H. Blumberg, J. Appl. Phys. 33, 1822 (1962).

[10]R. J. Duffy and H. Meissner, Phys. Rev. 147, 248 (1966).

[11]R. B. Dingle, Proc. Roy. Soc. (London) A201, 545 (1950).

[12]D. K. C. MacDonald, in *Encyclopedia of Physics*, edited by S. Flügge (Springer, Berlin, 1956), Vol. 14, p. 188.

[13]R. E. Miller and G. D. Cody, Phys. Rev. 173, 494 (1968).

[14]F. B. Hagedorn, Phys. Rev. Letters 12, 322 (1964).

[15]J. I. Gittleman and J. Bozowski, Phys. Rev. 135, A297 (1964).

[16]T. K. Hunt, Phys. Rev. 151, 325 (1966).